Enols of Carboxylic Acid Amides with β-Electron-Withdrawing Substituents

Jayanta Kumar Mukhopadhyaya, Stepan Sklenák, and Zvi Rappoport*

Contribution from the Department of Organic Chemistry and the Minerva Center for Computation Quantum Chemistry, The Hebrew University, Jerusalem 91904, Israel

Received June 17, 1999. Revised Manuscript Received November 18, 1999

Abstract: The effect of stabilizing enols of carboxamides by several two β-electron-withdrawing substituents was studied with the $R^1R^2CHCONHPh$ systems. When $R^1R^2CH_2$ = Meldrum's acid (MA), the solid-state structure is that of the enol $R^1R^2C{=}C(OH)NHPh$ (**7**). In $CDCl_3$ solution the structure is **7**, but there may be some exchange on the NMR time scale with a tautomer. B3LYP/6-31G** calculations show a significant preference for the enol $R^1R^2C{=}C(OH)NH_2$ (**12a**) (R^1R^2C = MA moiety) and a small preference for $(MeO_2C)_2C{=}C(OH)NHPh$ (**11b**) over the amide structures. However, solid **11** has the amide structure $(MeO_2C)_2$-CHCONHPh (**11a**). NMR spectra in $CDCl_3$ show >90% of **11a**, but a minor species, probably **11b**, is also present. In DMSO this species is not observed. The analogous dimedone-substituted anilide **10** exists both in the solid state and in solution as an enol of a ring carbonyl. Calculations show that $HC(CO_2Me)_3$ has a lower energy than its tautomeric enol. The effects of the push−pull structures of the enols on structural and spectrometric parameters, of the β-substituents, of the planarity of the system, of the acid derivative group (ester or anilide), and of the solvent as enol-stabilizing factors are discussed. Destabilization of the acid form contributes to the increased relative stability of the enols.

Introduction

In contrast with the extensive data on stable and short-lived enols of aldehydes and ketones,[1] enols of carboxylic acids and their derivatives (**1a**) are regarded as very unstable compared with their carbonyl analogues (**2a**) (eq 1).[2] Except for a few

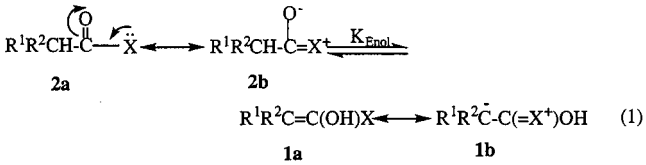

(1)

earlier reports,[3] only recently have some of these enols been suggested, detected, or prepared as short-lived intermediates,[4−6] and X-ray data of three derivatives were reported.[4g−i] Simple systems, i.e., neither highly activated electronically nor highly sterically crowded, were generated by nucleophilic addition to ketenes or by enolization of an α-hydrogen to the acid derivative function. They were observed by flash photolysis[5] or suggested as intermediates on the basis of kinetic and other evidence.[3,4] Similar nucleophilic addition to ketenes substituted by two bulky aryl groups (e.g., Ar = 2,4,6-$R_3C_6H_2$; R = Me, *i*-Pr) generated sufficiently long-lived enols which were observed by NMR before tautomerizing to the acid derivatives **2**.[6]

The relatively low K_{enol} values were ascribed to stabilization of the acid form by resonative electron donation from the heteroatom X (X = OH, OR, NRR′, OCOR″, halogen; cf. hybrid **2b**, eq 1).[2a] A similar resonative electron donation from X should also stabilize enols **1**. However, since oxygen is more electronegative than carbon, the contribution of **1b** to **1** when R^1 and R^2 are not strongly electron-withdrawing is lower than that of **2b** to **2**, and K_{enol} is much lower than when X = H.

(1) *The Chemistry of Enols*; Rappoport, Z., Ed.; Wiley: Chichester, 1990.

(2) For reviews on carboxylic acid enols, see: (a) Hegarty, A. F.; O'Neill, P. In ref 1, Chapter 10, p 639. (b) Kresge, A. J., *Chem. Soc. Rev.* **1996**, *25*, 275.

(3) (a) Zimmerman, H. E.; Cutshall, T. W. *J. Am. Chem. Soc.* **1958**, *80*, 2893. (b) Zimmerman, H. E.; Cutshall, T. W. *J. Am. Chem. Soc.* **1959**, *81*, 4305. (c) Ried, W.; Junker, P. *Justus Liebigs Ann. Chem.* **1967**, *709*, 85. (d) Lillford, P. J.; Satchell, D. P. N. *J. Chem. Soc. B* **1968**, 897. Poon, N. L.; Satchell, D. P. N. *J. Chem. Res., Synop.* **1983**, 182. However, see: Sikaly, H. R.; Tidwell, T. T. *Tetrahedron* **1986**, *42*, 2587. (e) Deno, W. C.; Billups, W. E.; Distefano, R. E.; McDonald, K. M.; Schneider, S. *J. Org. Chem.* **1970**, *35*, 278. (f) Quinkert, G. *Pure Appl. Chem.* **1973**, *33*, 285. (g) Montoneri, E.; Tempesti, E.; Giuffre, L.; Castold, A. *J. Chem. Soc., Perkin Trans. 2* **1980**, 662. (h) Hendon, J. E.; Gordon, A. W.; Gordon, M. *J. Org. Chem.* **1972**, *37*, 3184. (i) Kagan, J.; Tolentino, L.; Ettlinger, M. G. *J. Org. Chem.* **1975**, *40*, 3085.

(4) (a) Graham, L.; Williams, D. L. H. *J. Chem. Soc., Chem. Commun.* **1991**, 407. (b) March, J. *Advanced Organic Chemistry*, 4th ed.; Wiley: New York, 1992; p 590. (c) Williams, D. L. H.; Xia, L. *J. Chem. Soc., Perkin Trans. 2* **1992**, 747. (d) Nguyen, M. T.; Hegarty, A. F. *J. Am. Chem. Soc.* **1983**, *105*, 381. Hegarty, A. F.; Kelly, J. G.; Relihan, C. M. *J. Chem. Soc., Perkin Trans. 2* **1997**, 1175. (e) Williams, D. L. H.; Xia, L. *J. Chem. Soc., Perkin Trans. 2* **1993**, 1429. (f) Quinkert, G.; Kleiner, E.; Freitag, B.; Glenneberg, J.; Billhardt, U.; Cech, F.; Schmieder, K. R.; Schudok, C.; Steinmetzer, H.; Bats, J. W.; Zimmerman, G.; Dürner, G.; Rehm, D.; Paulus, E. F. *Helv. Chim. Acta* **1986**, *69*, 469. (g) Vilsmaier, E.; Joerg, K.; Mass, G. *Chem. Ber.* **1984**, *117*, 2947. (h) Bruce, M. I.; Walton, J. K.; Williams, M. L.; Skelton, B. W.; White, A. H. *J. Organomet. Chem.* **1981**, *212*, C35. (i) Galanski, M.; Keppler, B. K.; Nuber, B. *Angew. Chem., Int. Ed. Engl.* **1995**, *34*, 1103.

(5) (a) Andraos, J.; Chiang, Y.; Kresge, A. J.; Pojarlieff, I. G.; Schepp, N. P.; Wirz, J. *J. Am. Chem. Soc.* **1994**, *116*, 73 and references therein to Kresge's and Wirz's work. (b) Chiang, Y.; Jefferson, E. A.; Kresge, A. J.; Popik, V. V.; Xie, R.-Q. *J. Phys. Org. Chem.* **1998**, *11*, 610. (c) Wagner, B. D.; Arnold, B. R.; Brown, G. S.; Lusztyk, J. *J. Am. Chem. Soc.* **1998**, *120*, 1827.

(6) (a) O'Neill, P. J.; Hegarty, A. F. *J. Chem. Soc., Chem. Commun.* **1987**, 744. Allen, B. M.; Hegarty, A. F.; O'Neill, P.; Nguyen, M. T. *J. Chem. Soc., Perkin Trans.* 2 **1992**, 927. Allen, B. M.; Hegarty, A. F.; O'Neill, P. *J. Chem. Soc., Perkin Trans. 2* **1997**, 2733. (b) Frey, J.; Rappoport, Z. *J. Am. Chem. Soc.* **1995**, *117*, 1161; **1996**, *118*, 5169, 5182. (c) Frey, J.; Rappoport, Z. *J. Am. Chem. Soc.* **1996**, *118*, 3994. (d) Rappoport, Z.; Frey, J.; Sigalov, M.; Rochlin, E. *Pure Appl. Chem.* **1997**, *69*, 1933.

10.1021/ja992059f CCC: $19.00
Published on Web 02/05/2000

A number of recent theoretical calculations[7] and estimations[8] had confirmed that K_{enol} values for simple acid derivatives will be very low. The order of K_{enol} values for the parent $H_2C{=}C(OH)X$ (i.e., **1**, R^1, $R^2 = H$) as a function of X is H > alkyl > OCHO > Br ~ Cl > F > NH_2 > NMe_2 > OH, OMe.[7a] Hence, enols of anhydrides and amides have a better chance of being observed than enols of acids and esters.

Hybrid **1b** should be more important and K_{enol} higher when C_β carries negative charge delocalizing electron-withdrawing groups (EWGs) R^1 and R^2, as found for K_{enol} of simple enols **1**, X = H.[1] The effect of EWG on the stability of enols of acid derivatives was not directly investigated, although occasional reports had appeared (vide infra).

A possible complication is that the EWG may be the enolization site. For example, in a competitive enolization of an acid derivative (COX) with an aldehyde/ketone (COR), the enolization will be exclusively on the COR group, since the calculated K_{enol} value is 10 orders of magnitude higher for a COR than for a COX group.[7a] Indeed, $RCOCH(CO_2Et)_2$, $ArCH_2COCH_2COX$, X = OEt, NHPh, and β,β'-diketoesters enolize exclusively on the keto group.[9] Even with powerful EWGs, enolization to give **1** is not necessarily observed: $(O_2N)_2CHCOOEt$[10] and $HC(CO_2Me)_3$[11] are fully "ketonic".

A search of the Cambridge Structural Database (CSDB) for possible stable solid-state structures having the C=C(OH)NRR′ moiety reveal several such structures substituted by EWGs, such as nitromalonamide,[12] **3a**−**d**,[13,14a] and **4**.[14b] X-ray structures of

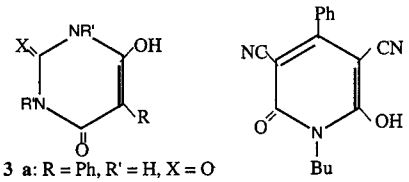

3 **a**: R = Ph, R' = H, X = O
b: R = OH, R' = H, X = O
c: R = NO_2, R' = H, X = O
d: R = H, R' = Et, X = S

4

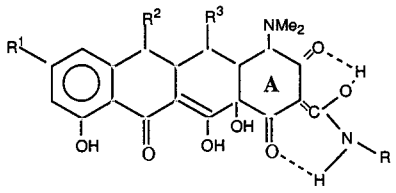

6a: R = R^1 = H, R^2 = H_2C=, R^3 = OH
6b: R = R^1 = H, R^2 = Me, R^3 = OH
6c: R^1 = OMe, R^2 = R^3 = H, R = *t*-Bu

tetracyclines usually display a O=C−CH(CONHR)−C=O moiety as part of ring A.[15] However, solid (**6a**)·HBr,[16a] (**6b**)·HCl,[16b] and (**6c**)[16c] appear as enols of amides **6** with an enolic OH hydrogen bonded to a neighboring carbonyl. Finally, solid pentakis(methoxycarbonyl)cyclopentadiene, $HC_5(CO_2Me)_5$, appears as an enol of ester.[17]

Consequently, two β-EWGs may stabilize enols of amides or esters in the solid. However, the structure in solution may be different and should be determined, and support by calculations is desirable. We describe below such a combined approach and an unequivocal example of an enol of amide.

Results

Synthesis and Structural Assignment of an Enol of Amide Stabilized by a Meldrum Acid Moiety. Pak et al.[18] reacted alkyl and aryl isocyanates with Meldrum's acid and wrote the products as the enols, but their spectra could also fit the amide form.[18] In a similar reaction with phenyl isocyanate (eq 2), we

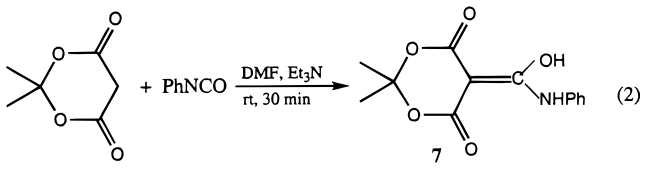

(2)

obtained 5-(α-phenylamino-α′-hydroxy)methylene Meldrum acid **7** in 74% yield. Its structural assignment in solution as **7** rather than the amide **8** is based on the room-temperature ^{1}H NMR ($CDCl_3$) spectrum: δ 1.78 (Me), 7.26−7.47 (Ph, m), 11.16 (1H, br), and 15.70 (<1H, br, rapidly disappearing on shaking the solution with D_2O). The data are consistent with assignment of the latter signals as NH and OH, respectively, i.e., with structures **7** and **9** but not with **8**. The δ 15.66 signal

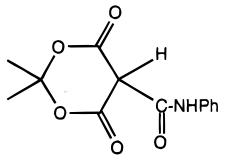

8

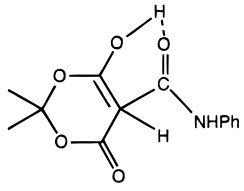

9

(1H) is broad at 240 K and shifts to δ 15.62 and becomes sharper at 223 K (Figure 1a). At 325 K, it is broad with intensity <1H. The ^{1}H NMR spectrum in $CCl_4/CDCl_3$ is similar. In CD_3CN or DMSO-d_6 the spectrum is similar, but no signal was observed at δ 15−16 (Figure 1b).

In the room-temperature ^{13}C NMR spectra in $CDCl_3$ and DMSO-d_6, most signals are at nearly the same δ values, but in DMSO-d_6 there are two signals of approximately the same intensity at 166.48 (m) and 168.37 (s) ppm, whereas three signals appear in $CDCl_3$ at 164.32 (br, low intensity), 169.15, and 170.84 (br, low intensity) ppm (Figure 2), and they become sharp at 223 K (Figure 2a, inset). At 325 K, the signals are at δ 169.26 and 170.82 with nearly identical intensity and δ 164.21

(7) (a) Sklenak, S.; Apeloig, Y.; Rappoport, Z. *J. Am. Chem. Soc.* **1998**, *120*, 10359 and refs 9 and 11 therein for work before 1996. (b) Gao, J. *J. Mol. Struct. (THEOCHEM)* **1996**, *370*, 203. (c) Rosenberg, R. E. *J. Org. Chem.* **1998**, *63*, 5562. (d) Rapoet, G.; Nguyen, M. T.; Kelly, S.; Hegarty, A. F. *J. Org. Chem.* **1998**, *63*, 9669. (e) Sung, K.; Tidwell, T. T. *J. Am. Chem. Soc.* **1998**, *120*, 3043. (f) Yamataka, H.; Rappoport, Z. Unpublished results.

(8) (a) Bok, L. D. K.; Geib, K. H. *Z. Phys. Chem. Abt. A.* **1939**, *183*, 353. (b) Guthrie, J. P. *Can. J. Chem.* **1993**, *71*, 2123. (c) Guthrie, J. P.; Liu, Z. *Can. J. Chem.* **1995**, *73*, 1395. (d) Amyes, T. L.; Richard, J. P. *J. Am. Chem. Soc.* **1996**, *118*, 3129.

(9) Toullec, J. In ref 1, Chapter 6, (a) p 323; (b) p 357; (c) p 361.

(10) Kissinger, L. W.; Ungnade, H. E. *J. Org. Chem.* **1958**, *23*, 1340.

(11) Guthrie, J. P. *Can. J. Chem.* **1979**, *57*, 1177.

(12) Simonsen, O.; Thorup, N. *Acta Crystallogr. Sect. B* **1979**, *57*, 1177.

(13) **3a**: de Mester, P.; Jovanovic, M. V.; Chu, S. S. C.; Biehl, E. R. *J. Heterocycl. Chem.* **1986**, *23*, 337. **3b**: Gavuzzo, E.; Mazza, F.; Carotti, A. Casini, G. *Acta Crystallogr. Sect. C* **1984**, *40*, 1231. **3c**: Bolton, W. *Acta Crystallogr.* **1963**, *16*, 950.

(14) (a) Bideau, J.-P.; Bravic, G.; Filhol, A. *Acta Crystallogr. Sect. B* **1977**, *33*, 3847. Bideau, J. P.; Huong, P.; Toure, S. *Acta Crystallogr. Sect. B* **1976**, *32*, 481. (b) Tranqui, D.; Vicat, J.; Thomas, M.; Pera, M. N.; Fillion, H.; Duc, C. L. *Acta Crystallogr, Sect. B* **1976**, *32*, 1724.

(15) For a discussion, see: Gilli, G.; Bertolasi, V. In ref 1, Chapter 13, pp 713−764, especially pp 736−740.

(16) **6a**: de C. T. Carrondo, M. A. A. F.; Matias, P. M.; Heggie, W.; Page, P. R. *Struct. Chem.* **1994**, *5*, 73. **6b**: Bordner, J. *Acta Crystallogr. Sect. B* **1979**, *35*, 219. **6c**: Glatz, B.; Helmchen, G.; Muxfeldt, H.; Porcher, H.; Prewo, R.; Senn, J.; Stezowski, J. J.; Stojda, R. J.; White, D. R. *J. Am. Chem. Soc.* **1971**, *101*, 2171.

(17) For a review, see: Bruce, M. I.; White, A. H. *Aust. J. Chem.* **1990**, *43*, 949.

(18) Lee, H. K.; Lee, J. P.; Lee, G. H.; Pak, C. S. *Synlett* **1996**, 1209.

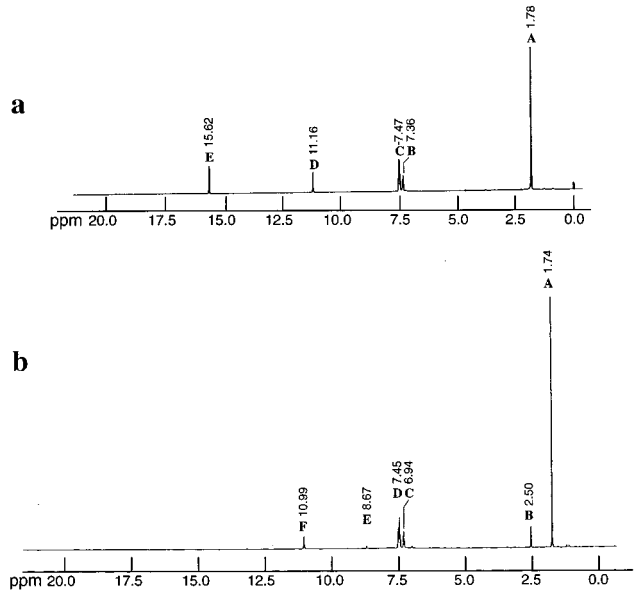

Figure 1. (a) ^{1}H NMR spectrum of **7** in $CDCl_3$ at 223 K: A, Me signal; B,C, Ph signal; D, N−H signal; E, O−H signal. (b) ^{1}H NMR spectrum of **7** in DMSO-d_6 at room temperature: A, Me signal; B, DMSO signal; C,D, Ph signal; E, ?; F, N−H signal.

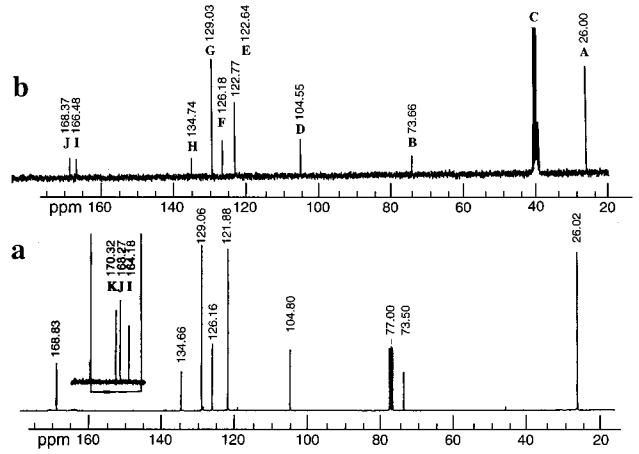

Figure 2. ^{13}C NMR spectrum of **7** at room temperature and in (a) $CDCl_3$ (inset at 223 K) and (b) DMSO: A, Me signal; B, C_β signal; C, DMSO signal; D, *C*Me$_2$ signal; E−H, Ph signals; I,J, CO, C_α signals.

is weaker. In 2,2-ditipyl-1-aminoethenols, C_α is at δ 156−157,[6d] and hence we ascribe the signal at δ 168.27 to C_α. The other two signals are due to the ester carbonyls.

In the coupled spectra C_β is at δ 75.31 (d, J = 7.5 Hz) (in ditipylacetic acid enol derivatives it is at δ 84−85.5[6c,d]), thus excluding structure **8** with a C−H coupled C_β. The δ difference between the vinylic carbons, $\Delta C_{\alpha\beta}$ = 93 ppm, is a higher value than that (74 ppm) found for the enols of ditipylacetamides.[6d] The aromatic signals are identified by their multiplicites, the lower intensity of C_p than C_o/C_m, and the NOESY spectrum: the higher field 1H triplet shows a cross-peak with δ 126.88; thus it is assigned as C_p. The 2H triplet at δ 7.39 shows a cross-peak with the ^{13}C signal at δ 122.59 and is assigned as C_o. The remaining 2H C_m signal correlates with δ 129.73. These assignments are used for all analogous cases. In the HMBC correlated spectrum, the N−H signal shows a cross-peak with C_o, and the O−H signal shows no cross-peak.

The ^{1}H NMR in $Cl_2CDCDCl_2$ at 245 K showed signals at δ 1.67 (6H), 7.09 (1H), 7.21−7.52 (4H), 10.99 (0.9H), 15.54-(0.09H). At 345−360 K, a new δ 2.11 signal (1.7H, br) appears,

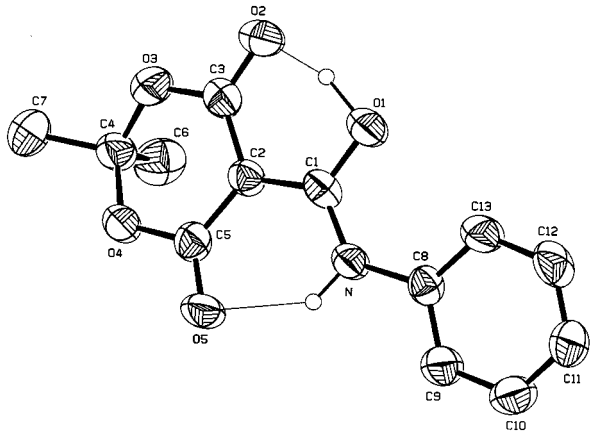

Figure 3. ORTEP drawing of **7**.

a small new signal appears at δ 8.80, and δ 15.58 (0.55H) is broad. On cooling a solution which stood 16 h at 345 K to room temperature, the signal at δ 2.11 still remains, and the aromatic region is more complex than that in the original room-temperature spectrum. The room-temperature ^{13}C NMR spectrum resembles that in $CDCl_3$. At 360 K, δ 164.56 disappears, and new signals appear at δ 30.77 and 129.18 and remain on cooling a sample which stood for 30 min at 360 K to room temperature. Hence, decomposition takes place at 345 and 360 K.

The ^{1}H NMR spectrum in CD_3CN at 220 K displayed OH, NH, Ph, and Me signals. The aromatic region showed several main signals at δ 7.35−7.57 and a small seven-line multiplet at δ 7.24−7.30 with 20% of the aromatic intensity. These and additional very small signals, e.g., at δ 11.4, indicate that more than one species may be present. In the ^{13}C NMR spectrum, C_α(m) is at δ 168.83, C_β(m) at δ 73.29, and δ(CO) at 163.36 (s) and 170.39 (s).

The δ values in the solid-state vacptppm and vacptppmnqs ^{13}C spectra are similar to those in $CDCl_3$ and DMSO and the approximate values predicted by Chemdraw 4.5 (cf. **7′**), suggesting a similar structure in solution and in the solid state.

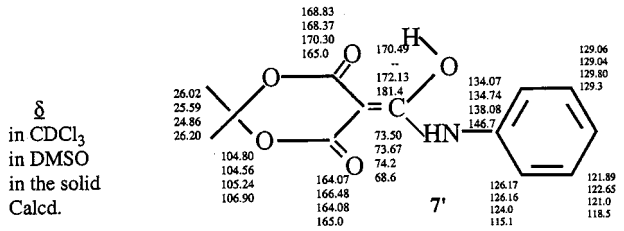

In $CDCl_3$ or DMSO-d_6 to which a 1:1 H_2O/D_2O mixture was added, the ^{13}C signals of **7** show deuterium-induced shifts. In $CDCl_3$, the *ortho* and *ipso* proton signals appear as two lines with spacings of 7 and 6 Hz, respectively.

X-ray Data of 7. The X-ray diffraction of solid **7** was determined. The ORTEP picture is given in Figure 3, selected bond lengths and angles are given in Table 1, and other bond lengths, angles, positional and thermal parameters and a stereoview are given in Tables S1−S3 and Figure S1 of the Supporting Information. The main features are the following: (a) The C1−C2 bond of 1.426(5) Å is longer than a C=C bond, shorter than a single bond, and in the range for "push−pull" enamines. (b) The C−N bond length is 1.333 Å. In a plot of C1−C2 vs C−N bond lengths in enamines, the point for **7** lies very close to the correlation line.[19] (c) The C5−O5 bond length of 1.221 Å is a normal value for a not strongly hydrogen bonded

Table 1. Selected Crystallographic Data for **7**

bond length, Å		angle, deg	
C1−C2	1.426(5)	C3−C2−C5	120.1(3)
C1−O1	1.300(4)	C1−C2−C3	117.2(3)
C1−N	1.333(4)	C1−C2−C5	122.4(3)
C3−O2	1.240(4)	N−C1−C2	121.5(3)
C5−O5	1.221(4)	C2−C3−O2	116.9(3)
C2−C3	1.420(5)	C2−C5−O5	126.1(3)
C2−C5	1.414(5)	C2−C5−O4	116.7(3)
C3−O3	1.341(4)	C2−C3−O3	118.6(3)
C5−O4	1.361(4)	O1−C1−N	118.4(3)
6 C−C in Ph	1.355(6)−1.385(6)	O1−C1−C2	120.1(3)
O1−H(1O1)	1.125	O1−H(1O1)−O2	158.24
O2−N(1O1)	1.385	N−H(1N)−O5	138.54
N−H(1N)	0.942		
O(5)−H(1N)	1.939		

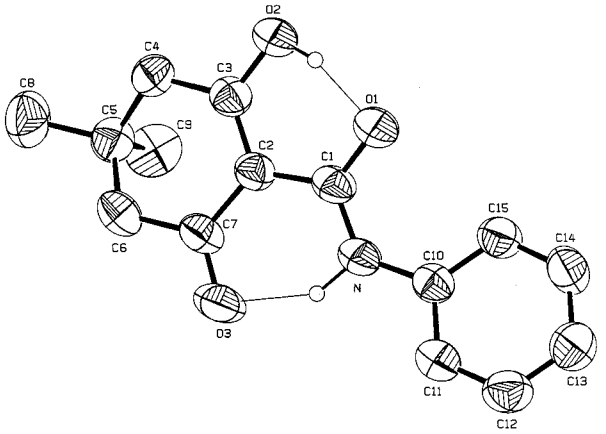

Figure 4. ORTEP drawing of **10c**.

C═O. The C3−O2 bond length of 1.240 Å is close to the normal value. The "amide carbonyl" C1−O1 bond is much longer (1.300 Å) and closer to a single C−O bond length, as expected for **7**. (d) The two C2−C═O bond lengths (1.414, 1.420 Å) are consistent with structure **7** having a $C_{sp2}-C_{sp2}$ bond. (e) The bond angles around C1 and C2 are 118.4°−122.4°, as expected for **7**. However, C1 and C2 are also sp^2-hybridized in **9**, where C1−C2 is a single bond. (f) The C2−C3−O3 angle of 118.6° fits either **7** or **9**. (g) The O1−O2 distance is 2.46 Å, the O1−H−O2 angle is 158.2°, and the O1−H distance is 1.125 Å, whereas the O2−H distance is significantly longer at 1.385 Å. This asymmetric nonlinear H-bond is consistent with form **7**, rather than with **9**. The N−O5 distance is 2.72 Å. The N−H bond length of 0.942 Å, the O5−H bond of 1.939 Å, and the N−H−O5 angle of 138.5° indicate a less symmetric, less linear, and weaker H-bond than the O2−H−O1 H-bond. (h) The system is nearly planar. H(N1) and O2 are ≤0.023 Å and C5 is 0.055 Å below the O1C1N plane, C2 and C3 are ca. 0.045 Å above it, and only O5 is significantly (0.22 Å) below it. The dihedral angle between planes O1C1N/C3C2C5 is 4.5°. Atoms C1, N, O2, and O5 are 0.14−0.15 Å, H(N1) is 0.10 Å, O1 is 0.23 Å, and H(O1) is 0.27 Å above the C3C2C5 plane.

The Dimedone Derivative, 10. (a) X-ray Data. The X-ray data of **10** show two crystallographically different molecules, mostly with similar bond lengths and angles. The structure is that of enol **10c**. The ORTEP drawing of one is given in Figure 4, selected bond lengths and angles are given in Table 2, and other bond lengths, angles, positional and thermal parameters and the stereoview are given in Tables S4−S6 and Figure S2 of the Supporting Information. The main features are the

(19) Oleksyn, B. J.; Stadnicka, K.; Sliwinski, J. In *The Chemistry of Enamines*; Rappoport, Z., Ed.; Wiley: Chichester, 1994; Chapter 2, p 87.

Table 2. Selected Crystallographic Data for **11**

bond length, Å		angle, deg	
C1−C2	1.470(5)	C3−C2−C5	118.8(3)
C1−O1	1.264(4)	C1−C2−C3	118.4(3)
C1−N	1.328(4)	C1−C2−C7	122.8(3)
C10−N	1.407(4)	N−C1−C2	118.7(3)
C3−O2	1.310(4)	C2−C3−O2	121.9(3)
C7−O3	1.246(4)	C2−C7−C6	118.1(3)
C2−C3	1.374(4)	C2−C7−O3	122.5(3)
C2−C7	1.444(4)	C2−C3−C4	114.4(3)
C3−C4	1.490(5)	O1−C1−N	121.8(3)
C6−C7	1.495(5)	O1−C1−C2	119.4(3)
6 C−C in Ph	1.371(5)−1.385(4)	O1−H(O2)−O2	162.0 (154)[a]
O2−H	1.07(5) [0.85(5)][a]	N−H(1N)−O3	143.4 (142.0)[a]
O1−H	1.62(5) [1.43][a]		
O3−H	1.76 [1.85][a]		
N−H	1.01(4) [(0.94(3)][a]		

[a] Data for a second crystallographic form.

following: (a) A normal $C_{sp2}-C_{sp2}$ C1−C2 single bond of 1.470 Å is found. (b) The C7−O3 bond is a short normal C═O bond, and the C3−O2 length of 1.310 Å is closer to a single bond length. The amide carbonyl C1−O1 bond length at 1.264 Å is normal. (c) C3−C4 and C6−C7 have normal sp^2-sp^3 C−C bond lengths. (d) The bond angles around C1 and C2 are 118.4°−122.8°, as expected. (e) The O1−O2 (O1′-O2′) distances are 2.44 (2.43) Å, and in the O−H−O moiety form O2−H (O2′−H′) = 1.07 (0.85) Å and the O1−H (O1′−H′) H-bond is 1.62 (1.43) Å; i.e., the structure is unequivocally **10c**. (f) The N1−O3 and N1′−N3′ distances are 2.65 Å. The O3−H(N1) distances are 1.76 and 1.85 Å in both forms. (g) The dihedral O1C1N/C3C2C7 angle is 4.7°.

(b) In Solution. The ^{1}H NMR spectrum of **10** in $CDCl_3$ displays signals for Me, two CH_2, Ph, NH, and a broad enolic singlet (rapidly exchanging with D_2O) at δ 1.15, 2.41 and 2.53, 7.17−7.56, 11.80, and 17.80. In DMSO-d_6, the spectrum is similar, but δ(OH) = 17.46. The spectrum is consistent with enolic forms **10b**−**d** but not with the "amide" **10a**. The ^{13}C NMR signals in $CDCl_3$, in DMSO-d_6, and in the solid state are at approximately the same δ values (cf. **10′**).

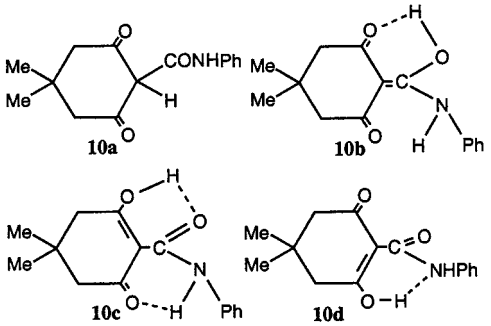

On shaking of a sample of **10** with D_2O in THF, the OH signal exchanges first, and the NH proton exchanges after a longer time, but the CH_2 groups do not exchange. After a relatively short exposure to D_2O, two deuterated samples, D1 with ca. 80% OD/30% ND, and D2 with ca. 90% exchanged OH/78% ND, were obtained. The residual OH signal is doubled to δ 17.79/17.81 singlets with 1:2 (D2) and 1:3 (D1) intensity ratios. The NH appears as two signals at δ 11.73/11.75 with ca. 7:3 (D1) and ca. 8:2 (D2) intensities.

For D1 in $CDCl_3$, the coupled ^{13}C NMR spectrum at 223 K displays the expected δ values and couplings expected for **10c**: δ 168.83 (br s, CONHPh), 101.74 (d, coupled with OH, C_β), 193.41 (t, ^3J = 6.8 Hz, coupled with CH_2, CO), and 194.17 (t,

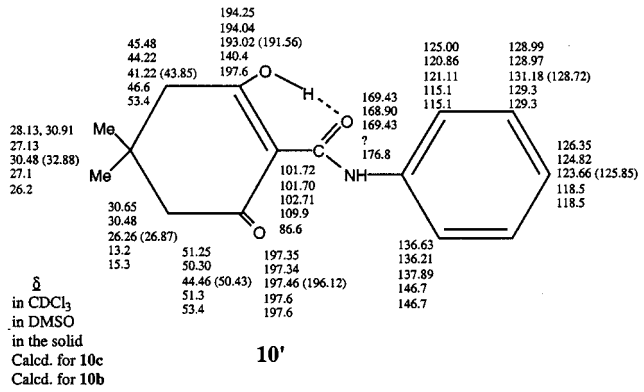

10'

^3J = 6.8 Hz, coupled with CH_2 and OH, C_α). At room temperature. the D1 sample shows low-field signals at δ 197.41 and 194.17 and a new one at δ 193.09. In D2, δ 194.17 nearly disappears, and δ 193.09, which is presumably an isotopically induced shifted signal, grows. The amide signal is also split to δ 168.90/169.29. At room temperature and at 223 K, the D1 spectrum shows splitting mostly of <0.12 ppm of many signals to pairs with ca. 3:1 intensities.

The IR spectrum in Nujol displays broad concentration-independent peaks at 3384, ca. 3187 (w) (OH and NH), 2820−2480 (H-bonded OH), 1720 (s), and 1654 (C═O) cm^{-1}. Sample D1 displays a broad peak at ca. 2320 cm^{-1} and three much less intense absorptions >2400 cm^{-1}. In $CHCl_3$, the peaks are at 3420−3400 (br), 1646−1640, and 1720 (weaker) cm^{-1}, with no signals at 2850−2400 cm^{-1}. Since for dimedone $\delta_{CO}(CHCl_3)$ = 1712 cm^{-1}, the data are consistent with structures **10b**−**d**.

The Malonic Ester Derivative, 11. The malonate **11** shows in $CDCl_3$ at room temperature signals at δ 3.86 (6H, Me), 4.49 (1H, CH), 7.12−7.58 (Ph, m), and 9.25 (small NH). The CH and NH signals exchange rapidly with D_2O. Significantly, two signals are observed at δ 17.05 (OH, 0.05H) and 3.81 (CH, 0.30H), as well as other aromatic and aliphatic signals (Figure 5). The two lower ^{13}C NMR signals at room temperature are at δ 159.60 and 166.10 (Figure S3a, Supporting Information). The IR spectrum in Nujol shows C═O peaks at 1751 and 1697 cm^{-1}. In DMSO-d_6, δ(CH) = 4.77, and δ(NH) = 10.33, but no OH signal (δ >11) is observed (Figure S3b).

$(MeO_2C)_2CHCONHPh$ **11a**

$(MeO_2C)_2C{=}C(OH)NHPh$ **11b**

$(MeO_2C)_2CHC(OH){=}NPh$ **11c**

$MeO_2CC(CONHPh){=}C(OH)OMe$ **11d**

The data are consistent with the presence of ca. 95% of the amide **11a** in $CDCl_3$ solution. The minor isomer (ca. 5%) is an enol, either **11b**, **11c**, or **11d**. The **11a** ⇌ **11b** (or **11c** or **11d**) equilibrium is rapid, judging by the rapid exchange of the CH signal with D_2O. The exchange was slower at 220 K, where a signal at δ 9.61 (N−H of **11a**) and two 0.05−0.02H signals at δ 11.9 and 17.2 (presumably the N−H and O−H of **11b**, **11c**, or **11d**) are observed. These and the appearance of several small signals at δ 3.78−3.94, close to the major MeO signal (Figure 6), suggest that more than one of the species **11b**, **11c**, or **11d** is present in small percentages.

Crystal Structure of 11. The crystal structure of **11** was determined by X-ray diffraction as that of the amide **11a**. The ORTEP drawing is in Figure 7, selected bond lengths and angles are in Table 3, and other bond lengths and angles, thermal and

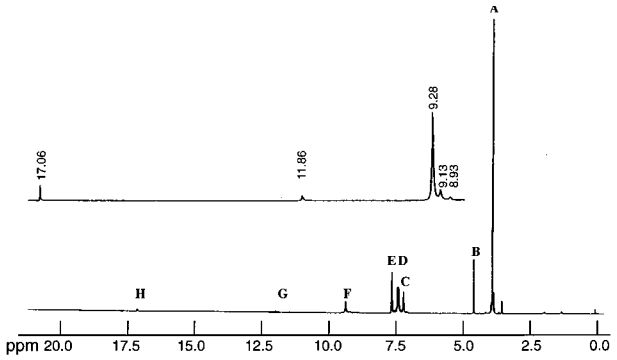

Figure 5. ^1H NMR spectrum of **11** in $CDCl_3$ at room temperature. Signals A−F are those of **11a**. Bottom, full spectrum: A, Me signal; B, C−H signal; C−E, Ph signals; F, N−H signal. Signals G and H are the N−H and O−H signals of an isomer (**11b**, **11c**, or **11d**). Top: Expansion of the range of the F, G, and H signals.

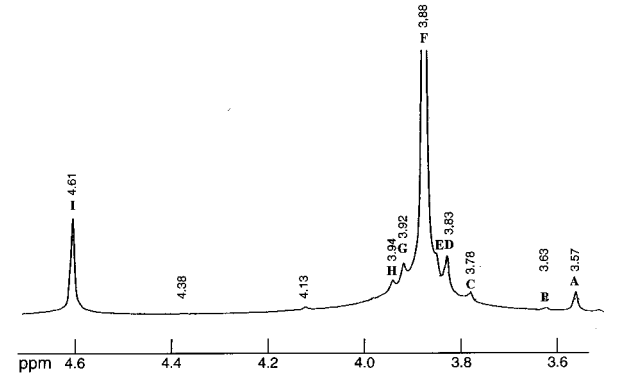

Figure 6. Aliphatic range of the ^1H NMR spectrum of **11** in $CDCl_3$ at 220 K. Signals F and I are those for the MeO and CH groups of **11a**. Signals A−E, G, and H are due to MeO groups of two or more of the minor isomers (**11b**, **11c**, or **11d**).

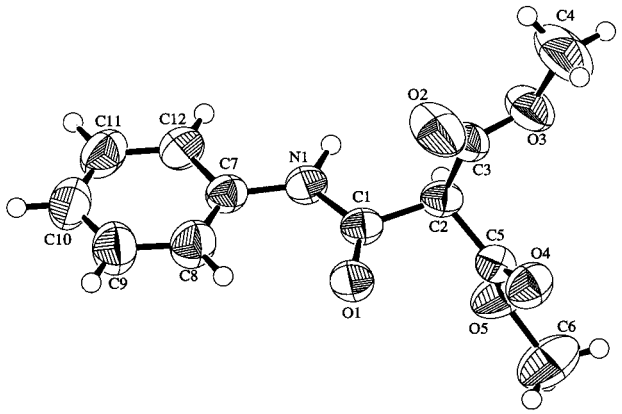

Figure 7. ORTEP drawing of **11a**.

positional parameters, and the stereoview are in Tables S7−S9 and Figure S4 in the Supporting Information. There are three independent molecules, and in one (designated with ″) C6 is disordered. One molecule displays a H-bonded homopolymeric network where O1 of one molecule is H-bonded to the NH of another, whose O1 is H-bonded to the NH of a third one (Figure S5, Supporting Information). The two other types of molecules form a similar heteropolymer array, with a repeating second molecule−third molecule H-bonded unit (Figure S6). The C1−O1 (and C1′−O1′, C1″−O1″) bond length of 1.216(4) Å (1.25-(4), 1.216(4) Å) is definitely a C═O bond, and C1−C2 (and C1′−C2′, C1″−C2″) of 1.528(5) Å (1.521(3), 1.520(5) Å) is a single bond.

Chart 1. Relative Energies of **12a**−**e**

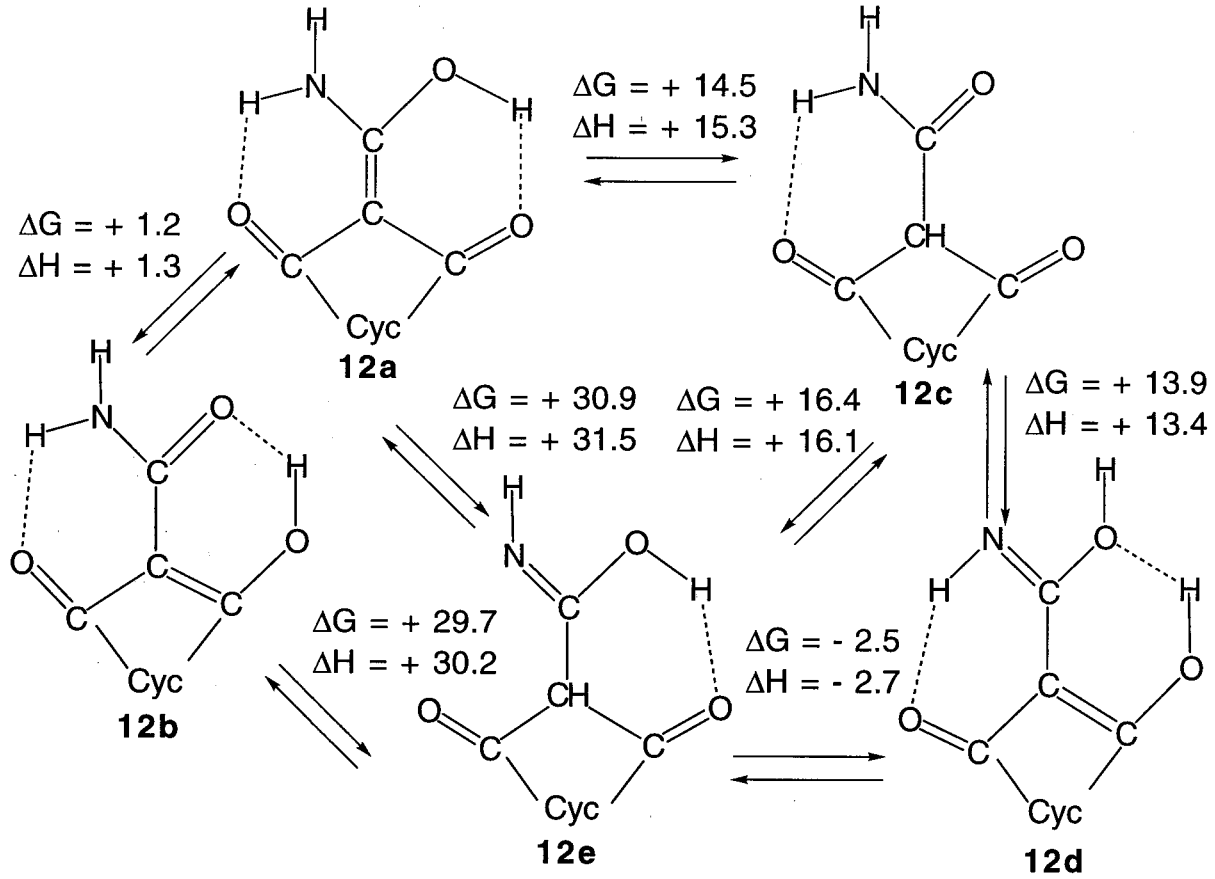

Table 3. Bond Lengths and Angles in Solid **12**[a]

bond length, Å		angle, deg	
C1−C2	1.528(5)	C1−C2−C3	110.6(3)
C1−O1	1.216(4)	C1−C2−C5	109.3(3)
C2−C3	1.507(5)	N1−C1−C2	113.5(3)
C2−C5	1.499(5)	C3−C2−C5	109.3(3)
C3−O2	1.175(5)	O1−C1−C2	121.3(3)
C3−O3	1.318(5)	C1−N1−C7	127.9(3)
C4−O3	1.446(6)	N1−C7−C12	116.4(3)
C5−O4	1.200(4)	6 inter-ring CCC	120.0(4) ± 0.8
C5−O5	1.315(4)		
C6−O5	1.467(6)		
C1−N1	1.348(5)		
C7−N1	1.423(5)		
6 C−C in Ph	1.376(6) ± 0.009		

[a] Data for one independent molecule are given. The values for the other two molecules are very similar.

α-Aryl and α-Alkyl Malonate Esters. Since diethyl benzylmalonate was reported to be 13% enolic,[20] we searched for enols in systems $RCH(CO_2Et)_2$, R = Ph, $PhCH_2$ or $Ph_3CCH(CO_2Me)_2$. Their ^1H NMR spectra in $CDCl_3$ are consistent with the diester structures.

Theoretical Calculations. Relative stabilities of various isomers were calculated for the Meldrum acid derivative **12**,

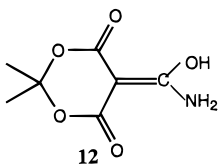

12

the diester **11**, and the triester **13** by using the density functional theory hybrid method (B3LYP/6-31G**).[21] Full optimization was performed, and vibrational frequencies, zero point energies (ZPE), and ΔH and ΔG values (E = electronic energy; $H = E + E_{ZPE}$; G = Gibbs free energy) were calculated.

Compound 12. The calculations show five different distinct species of **12** (**12a**−**e**, Chart 1, where "Cyc" = O−CMe_2−O part of the Meldrum's acid (MA) moiety), each having several stable conformers. Geometries of **12a**−**c** are in Chart 2, and selected optimized dihedral angles and the structures of **12d** and **12e** are in Table S10 and Figure S7 in the Supporting Information. The most stable isomer is the enol of amide **12a**, which has only two stable conformers: the intramolecularly H-bonded *syn* form is 19.9 kcal/mol more stable than the *gauche* form (C=C−O−H dihedral angle = −165.5°). Isomer **12b**(*syn*), with an enol on the ring ester carbonyl, is less stable by 1.2−1.3 kcal/mol than **12a**. **12b** has two conformers: the intramolecularly H-bonded *syn* is favored by 20.6 kcal/mol over the *anti* form (C=C−O−H angle = 177.6°). The **12a**/**12b** interconversion requires a shift by a fraction of an angstrom of the enolic hydrogen between the two oxygens.

Third in stability is the amide form **12c**, whose most stable

(20) Skarzewski, J. *Tetrahedron* **1989**, *45*, 4593. However, it seems that the compound meant is diethyl benzoylmalonate. Tarbell, D. S.; Price, J. A. *J. Org. Chem.* **1957**, *22*, 245.

(21) (a) Frisch, M. J.; Trucks, G. W.; Schlegel, H. B.; Gill, P. M. W.; Johnson, B. G.; Robb, M. A.; Cheeseman, J. R.; Keith, T. A.; Petersson, G. A.; Montgomery, J. A.; Raghavachari, K.; Al-Laham, M. A.; Zakrzewski, V. G.; Ortiz, J. V.; Foresman, J. B.; Cioslowski, J.; Stefanov, B. B.; Nanayakkara, A.; Challacombe, M.; Peng, C. Y.; Ayala, P. Y.; Chen, W.; Wong, M. W.; Andress, J. L.; Replogle, E. S.; Gomperts, R.; Martin, R. L.; Fox, D. J.; Binkley, J. S.; Defrees, D. J.; Baker, J.; Stewart, J. P.; Head-Gordon, M.; Gonzalez, C.; Pople, J. A. *GAUSSIAN 94*, Revision C.2; Gaussian Inc.: Pittsburgh, PA, 1995. (b) Hehre, W. J.; Radom, L.; Schleyer, P. v. R.; Pople, J. A. *Ab Initio Molecular Orbital Theory*; Wiley: New York, 1986. (c) Becke, A. D. *J. Phys. Chem.* **1993**, *98*, 5648. (d) Lee, C.; Yang, W.; Parr, R. G. *Phys. Rev. B* **1988**, *37*, 785.

Chart 2. Calculated Structures of **12a**−**e**

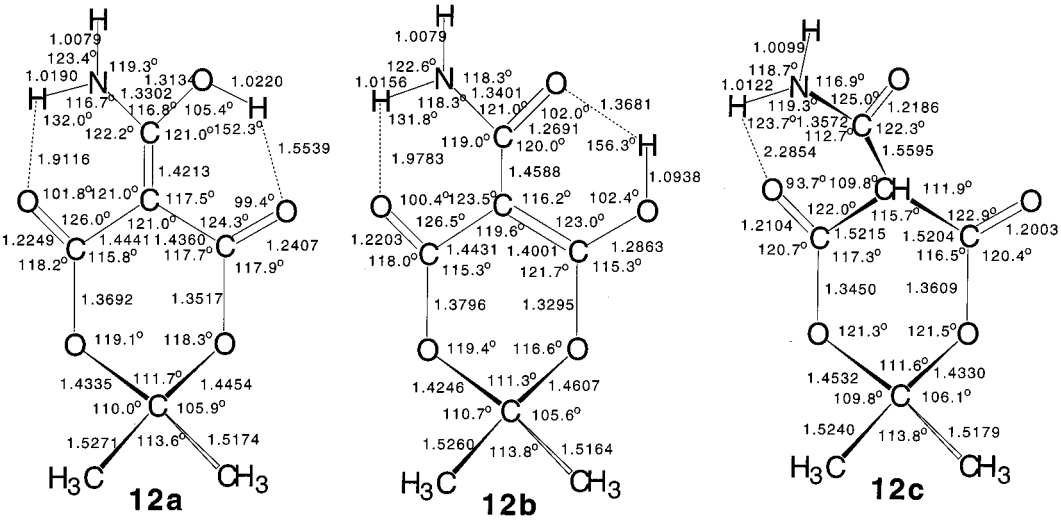

conformer is ca. 15 kcal/mol less stable than **12a**. The imino form **12d** is less stable than **12c** and **12a** by ca. 13 and 29 kcal/mol, respectively. The least stable isomer is the enamine **12e**; its most stable calculated conformer is ca. 16 kcal/mol less stable than **12c** and ca. 3 kcal/mol than **12d**.

12a, **12b**, and **12d** have an approximately planar N(O)C═C(CO_2)$_2$ moiety with a C(O═)−C−C(═O)−O dihedral angle of 5−8°. **12c** and **12e** have a boat structure with Me_2C and $CHCONH_2$ (or CHC(OH)═NH) groups above the central plane containing the two ester groups. The chair conformers have higher energies. The OO distances relevant to the hydrogen bonds in **12a**, **12b**, and **12d** are 2.50, 2.41, and 2.55 Å, respectively.

The solvent effects on ΔE [(**12a**) − (**12b**)] were briefly investigated by applying SCRF = SCIPCM calculations,[22] including geometry reoptimization, taking the ZPE from the gas-phase calculations. The geometry changes and ΔE[(**12a**) − (**12b**)] are small. **12a** is more stable than **12b** by 1.5 and 2.1 kcal/mol in heptane (ϵ = 1.92) and in water (ϵ = 78.39), respectively.

An attempt to locate the transition state for the proton transfer between **12a** and **12b** ended in either structure **12a** or **12b**. When equal O−H distances were used, we obtained a "transition state" with one negative frequency of 847 cm^{-1} corresponding to the hydrogen migration between the oxygens, whose energy was that of **12a**. Consequently, the barrier to the process is close to 0 kcal/mol.

Compound 11. There are many conformers of the isomers of **11**. For enol **11b** we calculated four conformers with *syn* C═C−O−H and *anti* C═C−N−Ph moieties which differ in the relative orientation of the C(═O)O and the C═C groups. Four conformers of **11a** were calculated. The relative energies (in kcal/mol) (Chart 3) of the most stable structures (Chart 4) are **11b** (0) > **11a** (5.6) > iminoenol (**11c**) (20.2). We failed to find a minimum corresponding to the ester enol **11d**.

Compound 13. The energies of **13a** and its enol **13b** were also calculated. The geometries are given in Chart 5. **13a** is favored over **13b** by 3.9 kcal/mol (Chart 6).

$CH(CO_2Me)_3$ $(MeO_2C)_2C{=}C(OH)OMe$
13a **13b**

(22) Foresman, J. B.; Keith, T. A.; Wiberg, K. B.; Snoonian, J.; Frisch, M. J. *J. Phys. Chem.* **1996**, *100*, 16098.

Chart 3. Relative Energies of **11a**−**c**

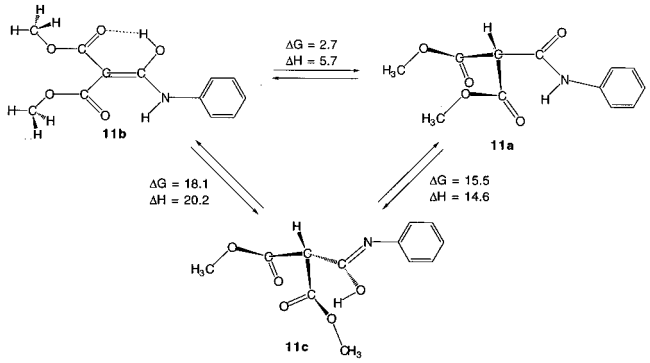

The effects of β-dicarbomethoxy substitution on the enol and the ester for both **11** and **13** and the imine in system **11** are deduced from the isodesmic reactions 3a−7a and 3b−7b.

	ΔH, kcal/mol	
$(MeO_2C)_2C{=}C(OH)NHPh + CH_4 \rightleftharpoons$ $H_2C{=}C(OH)NHPh + H_2C(CO_2Me)_2$	+37.0	(3a)
$(MeO_2C)_2CHC(NHPh){=}O + CH_4 \rightleftharpoons$ $MeC(NHPh){=}O + H_2C(CO_2Me)_2$	+3.1	(4a)
$(MeO_2C)_2CHC(OH){=}NPh + CH_4 \rightleftharpoons$ $MeC(OH){=}NPh + H_2C(CO_2Me)_2$	+0.6	(5a)
$(MeO_2C)_2C{=}C(OH)OMe + CH_4 \rightleftharpoons$ $H_2C{=}C(OH)OMe + H_2C(CO_2Me)_2$	+24.4	(6a)
$(MeO_2C)_2CHC(OMe){=}O + CH_4 \rightleftharpoons$ $MeC(OMe){=}O + H_2C(CO_2Me)_2$	−1.4	(7a)
$(MeO_2C)_2C{=}C(OH)NHPh + H_2C{=}CH_2 \rightleftharpoons$ $H_2C{=}C(OH)NHPh + H_2C{=}C(CO_2Me)_2$	+29.1	(3b)
$(MeO_2C)_2CH(NHPh){=}O + H_2C{=}CH_2 \rightleftharpoons$ $MeC(NHPh){=}O + H_2C{=}C(CO_2Me)_2$	−4.8	(4b)
$(MeO_2C)_2CHC(OH){=}NPh{+}H_2C{=}CH_2 \rightleftharpoons$ $MeC(OH){=}NPh + H_2C{=}C(CO_2Me)_2$	−7.3	(5b)
$(MeO_2C)_2C{=}C(OH)OMe + H_2C{=}CH_2 \rightleftharpoons$ $H_2C{=}C(OH)OMe + H_2C{=}C(CO_2Me)_2$	+16.5	(6b)
$(MeO_2C)_2CHC(OMe){=}O + H_2C{=}CH_2 \rightleftharpoons$ $MeC(OMe){=}O + H_2C{=}C(CO_2Me)_2$	−9.3	(7b)

Discussion

The calculated very large energy preference of the parent acid derivative structure over its enol form[7] indicates the need for a significant driving force to overcome this difference. Both calculations and NMR studies of β,β-di(bulky)aryl enols of acid derivatives[6,7f] indicate that an increased steric bulk is still an

Chart 4. Calculated Structures of **11a**−**c**

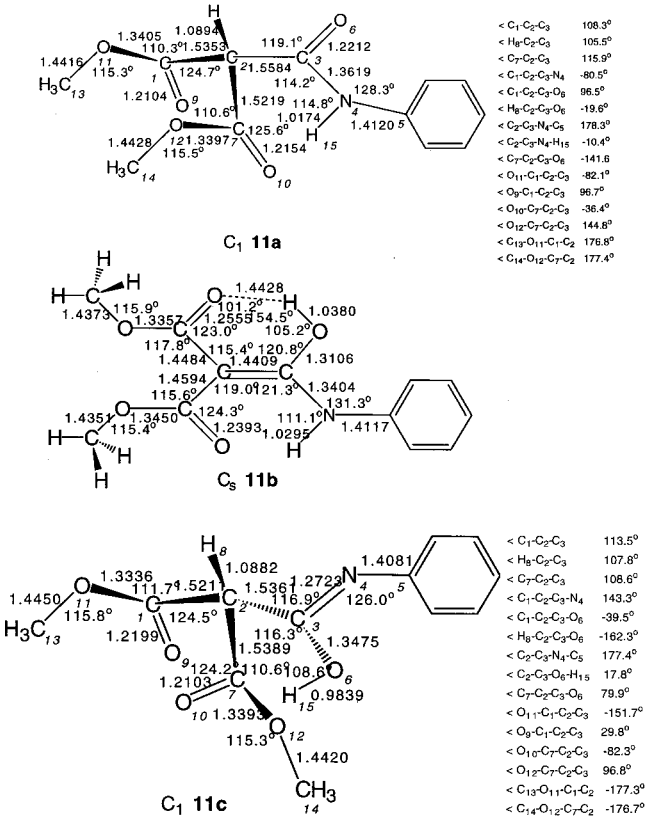

Chart 5. Calculated Structures of **13a** and **13b**

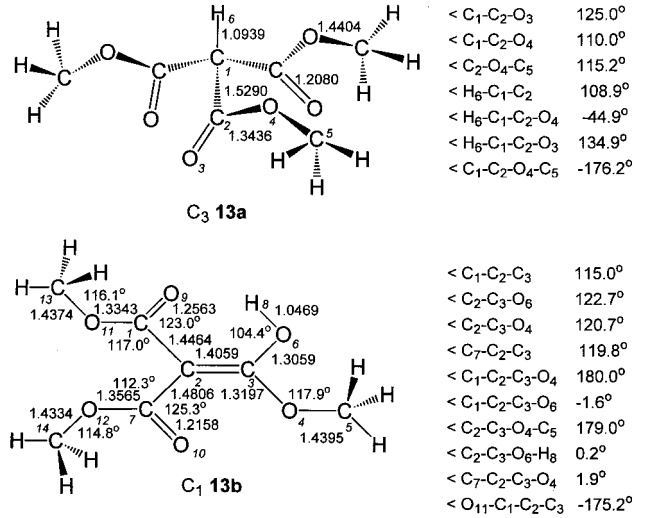

insufficient driving force. However, from the scattered X-ray data, a sufficient stabilization can be achieved by substitution with EWGs and via intramolecular H-bonding. The evidence for short-lived unobservable enols indicate that *two* strongly β-EWGs are required but not always sufficient for observing an enol of an acid derivative. This approach is used in this work.

Enols in the Solid State: Comparison with Calculations. We will discuss separately the situation in the solid state, which is not ambiguous, and that in solution. The X-ray structures for three $(EWG)_2CHCONHPh$ systems display different structural

Chart 6. Relative Energies of **13a** and **13b**

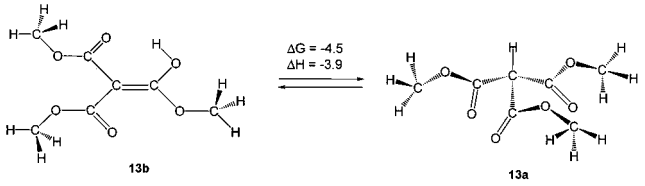

types, demonstrate potential problems, and give a glimpse of the substituent effects. They also demonstrate unique features of our enols, derived from the presence of the push−pull interaction of the α- and β-substituents.

(a) **The Meldrum Acid Systems 7 and 12.** The O(1)−H and O(2)−H distances indicate an enol structure for the solid MA derivative **7**. Planarity of the $(O{=}C)_2C{=}C$ moiety increases the resonance stabilization of the enol (cf. **1b**). Although $K_{enol}(CH_3CONH_2) > K_{enol}(CH_3CO_2CH_3)$,[7a] **7** is not necessarily more stable than the enol of ester isomer **9**, since NH_2 is a better resonative electron-donating group than OMe and a β-CO_2R group delocalizes negative charge better than β-CONHPh.

The calculations enable comparison of the observed structure of the N−Ph **7** (Figure 3) with that calculated (Chart 1) for the N−H **12a** and with experimentally nonavailable isomers. The data for **7** and **12a** show only small differences: <0.01 Å for the C1−C2, C1−N, C1−O1, C5−O5, C3−C2, and C5−O4 bonds, and ≥0.03 Å for the C2−C3, C2−C5, and C3−O3 bonds. Higher deviations (obsd vs calcd in Å) for the O1−H(1O) (1.125, 1.022), O3−H(1O) (1.385, 1.556), N−H(1N) (0.942, 1.019), and O(5)−H(1N) (1.939, 1.912) bonds reflect the higher errors associated with bonds to hydrogen. The angles differ by <3°. The differences between **7** and **12b** are larger, except for the similar C5−O5, C2−C5, and N−H(1N) bond lengths in both structures.

The calculated structures and energies of **12a** and **12b** do not differ much. Both have a six-membered enone-containing ring with one intramolecular H-bond. A proton shift by 0.46 Å between two oxygens converts **12a** to **12b**. The differences of the formal single and double bonds lengths in this ring are smaller than expected: 0.036 and 0.037 Å for the C=C/C−C bonds and 0.046 and 0.042 Å for the C=O/C−O bonds. The energy difference of slightly more than 1 kcal/mol means that both could coexist. The difference is remarkably smaller than the 19.9 kcal/mol preference of the *syn* over the *gauche* conformer of **12a**. Indeed, a *syn* arrangement is observed for **7**.

The 15 and 16 kcal/mol higher stability, respectively, of both **12a** and **12b** over the amide form **12c** contrasts the ΔG preferences of the "keto" forms CH_3CONH_2 and CH_3CO_2Me over their enols by 28.9 and 30.3 kcal/mol at B3LYP/6-31G**//B3LYP/6-31G**.[7k] Hence, the two cyclic ester groups enormously stabilize the enol relative to the amide form by ca. 44 kcal/mol. The $CH_3CONH_2/CH_3C(OH){=}NH$ difference of 14 kcal/mol[7k] resembles the **12c**/**12e** difference of 16.4 kcal/mol, indicating a small effect of the β-ester groups on the keto/imine equilibria.

(b) The "Amide" Derivative 11. When the *E* conformation of the ester groups of **7** disappears, a large part of the relative stabilization of the enol is lost. The solid open-chain β-diester with a *Z* conformation of the ester moieties exists as the amide form **11a**. However, the calculation that **11b** is 5.6 kcal/mol more stable than **11a** predicts that solid **11** will exist as the enol. The discrepancy may be due to the fact that not all the conformers of both **11a** and **11b** were calculated. For **11b**, all the highly stable *syn* C=C−O−H conformers were calculated, and we believe that we did not miss the most stable conformer.

However, if the most stable conformer of **11a** was missed, the calculated K_{enol} would be higher than the "real" one. This is unlikely since the use of the experimental data for solid **11a** led to a conformer identical to a previously calculated one. Packing forces in solid **11a** could also be responsible for the discrepancy.

(c) Tricarbomethoxymethane, 13. Of the two isomers of **13**, the amide form **13a** is 4.5 kcal/mol more stable than the enol **13b**. In **13b**, the resonative system O4O6C3C2C1(═O9) is nearly planar, with a 28.6° twist of the MeO_2C group *cis* to OMe from this plane. Hence, even with the extensive conjugation, reflected by the long C═C bond of 1.406 Å and the short C−C(═O) bonds of 1.446 Å to the planar CO_2Me group and 1.481 Å to the twisted one, two β-ester groups are insufficient for a significant enolization of a third one.

(**d) The Dimedone-Substituted Anilide.** The diketo-activated cyclic analogue of **7** enolizes on a ring carbonyl rather than on the amide group. Since the calculated K_{enol} values of CH_3COR are $\geq 10^7$ larger than that of CH_3CONH_2,[7a] the order of preference should be **10c** or **10d** ≫ **10b** > **10a**. Indeed, the X-ray structure is that of **10c**. The enol to enol interconversion **10c** ⇌ **10a** requires a proton shift from O2 to O1.

Enols in Solution. The isomeric composition in solution can differ from the solid-state structure due to crystal-packing forces and differential solvation. Several isomers can coexist in solution and may undergo a rapid exchange. The strongly resonative electron-donating NHPh and OH groups on C1 and the strong CO_2R or CO EWGs on C2 stabilize the enol and give C1−C2 a partial single bond character (cf. **1b**). Structural and spectrometric parameters may then resemble those expected for the amide form.

Structural Parameters. The C1−C2 bond in solid **7** is longer and the C1−N bond shorter than their values in enamines, which in frequency vs bond length histograms give maximum values of 1.35 and 1.39 Å, respectively.[19] In the CSDB, in 17 of the 206 enaminoesters $RO_2CC(R')═C(R'')NR'''R^{IV}$, the C1−C2 bonds are longer than 1.400 Å and the group R′ is able to resonatively delocalize the negative charge on C2 in the dipolar structure. The model closer to **7** is $PhC(NRR')═C(CHO)CO_2$-Et (C1−C2 1.409 Å, C−N 1.356 Å),[23] and the extreme case is $RPhNC(R)═C(CO_2Me)COCO_2Me$ (C1−C2 1.470 Å, C−N 1.335 Å).[24] Hence, the data for **7** are normal, when the additional resonative electron donation by the OH group on C1 is considered.

Similar changes are observed in the calculated structures **11b** and **13b**, where the C═C and ═C−C(═O) bond lengths are 1.44, 1.448, and 1.459 Å and 1.40, 1.446, and 1.480 Å, respectively. In the amide analogues these bonds have normal lengths. The observed C1−C2 and C1−N bond lengths are 1.528 and 1.348 Å in **11a**, and the calculated C−C bond length in **13a** is 1.5290 Å. In contrast, in enol **10**, C1−C2 is 1.470 Å, C1−O1 is 1.264 Å, and C1−N is 1.328 Å, and these values differ significantly from those for enol **7**.

IR Frequencies. The longer C1−C2 bond length and the partial double bond character of the β-EWG affect the IR frequencies. Compared with $\nu_{max} = 1715-1730$ cm^{-1} for α,β-unsaturated CO or CO_2Et groups lacking α-electron-donating groups,[25a] ν_{max} should appear at lower wavelengths. Indeed, for **7** and **11**, $\nu_{max}(CHCl_3) = 1697$ cm^{-1}.

Chemical Shifts. Due to the dipolar character, δC_α should be at a much lower field and δC_β at a much higher field than $\delta^{13}C = 105-145$ in simple ethylenic carbons.[25b] In **11**, $\delta C_\alpha =$ ca. 168 and $\delta C_\beta =$ ca. 74. This raises assignment problems since C_α of the enol can be in the CO range of esters and amides.

The δ^1H(OH) at $\delta > 15.5$ in **7**, **11b**, and **10c** indicates the presence of a strong H-bond to the enolic hydrogen[26] in a six-membered ring which includes this bond. This resembles the situation for the stable enols of β-diketones.

Observable Enols in Solution. $CDCl_3$ and DMSO-d_6 were used as low-polarity and dipolar aprotic solvent, respectively. When low solubility, signals overlap, and inaccessible temperatures were encountered, $Cl_2CDCDCl_2$ and CD_3CN were used instead. Significant differences in the behavior in the two solvents were observed.

(a) The MA Derivative. The calculated **12a/12b** energy difference suggests that **7** and **9** may coexist in solution. Whereas the Me, Ph, and NH signals in $CDCl_3$ or $Cl_2CDCDCl_2$ are at the expected δ^1H values for either isomer **7**−**9**, the rapidly exchanging δ 15.70 signal in $CDCl_3$ and the lack of an aliphatic C−H signal exclude structure **8**. The uncoupled C_β, the two δ^{13}C ester signals, the H−C correlation spectra, and the similarity of the solution and solid NMR spectra exclude structure **9**.

The large $\Delta C_{\alpha\beta}$ of 93 ppm is consistent with the push−pull structure **7**. For comparison, we measured the ^{13}C NMR spectra of the analogues **14a**[27] and **14b**,[28] having two resonatively electron-donating α-substituents. For **14a**, $\delta^{13}C(CDCl_3$, rt) =

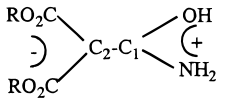

7''

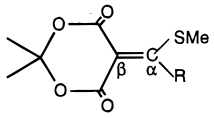

14a: R = SMe
14b: R = N[(CH$_2$)$_2$]$_2$O (morpholino

102.74 (s, C_β), 159.68 (s, COOR), and 192.36 (heptet, $J = 5$ Hz, C_α), $\Delta C_{\alpha\beta} = 89.4$ ppm. For **14b**, δ^{13}C 79.11 (C_β),161.64 (CO_2R), and 185.88 (C_α), $\Delta C_{\alpha\beta} = 106.8$ ppm. Hence, C_β of **14a** is close to C_β in **7**, and the high $\Delta C_{\alpha\beta}$ values fit structure **7** and indicate that $\delta^{13}C_\alpha$ can be in the range of a carbonyl group or even lower.

The low intensity and broadening of the room temperature CO signals and the intensity increase at 223 K may indicate an exchange with an isomeric species such as **9** (cf. Chart 1). Since the ^{13}C−H correlation does not show cross-peaks corresponding to **9**, if it is present in the mixture its concentration must be low.

The spectra of **7** in CD_3CN resemble those in $CDCl_3$. Due to the unobserved OH and C_α signals at room temperature in DMSO-d_6, exchange with **9** is more probable than in $CDCl_3$, but the similarity of the δ^{13}C values of the solid and in DMSO-d_6 support structure **7**.

(b) The Dimedone Derivative. The similar spectra of **10** in solution and in the solid state fit structure **10c**. We attribute one of the low-field signals in the ^{13}C NMR spectra to C_α.There is no evidence for the presence of other enols in solution.[29]

(c) The Malonic Ester Derivative 11. The ^{1}H spectrum of **11** in $CDCl_3$ is that of the amide form **11a**. However, the additional small signal at δ 17.05 (OH), several MeO signals at ca. δ 3.81 (Figure 6), and N−H signals (Figure 5) indicate

(23) Freeman, J. P.; Duchamp, D. J.; Chidester, C. D.; Slomp, G.; Szmuszkovicz, J.; Raban, M. *J. Am. Chem. Soc*. **1982**, *104*, 1380.
(24) Butler, R. N.; Gillan, A. M.; Lysaght, F. A.; McArdle, P.; Cunningham, D. *J. Chem. Soc., Perkin Trans. 1* **1990**, 555.
(25) Field, L. D.; Sternhell, C.; Kalman, J. R. *Organic Structures from Spectra*, 2nd ed.; Wiley: Chichester, 1995; (a) p 15; (b) p 63.
(26) Perrin, C. L.; Nielson, J. B. *Annu. Rev. Phys. Chem*. **1997**, *48*, 511.
(27) Huang, X.; Chen, B. C. *Synthesis* **1986**, 967.
(28) Salim, H., unpublished results.
(29) Mukhopadhyaya, J.; Rappoport, Z., unpublished results.

also the presence of ca. 5% of at least two enolic species, presumably those of an amide (**11b**) and of an ester (**11d**), since **11c** has a relatively high energy. Due to *E*/*Z* isomerism, **11d** can show four MeO signals, whereas **11b** should display two MeO groups which are in different environments. Since the ^{13}C NMR spectrum displays only signals of **11a** and the IR peaks at 1751 and 1697 cm^{-1} are consistent with the ester and amido carbonyls of **11a**, the other isomers are, indeed, present to a low extent.

The rapid disappearance of the methine proton of **11a** in $CDCl_3/D_2O$ at room temperature suggests that a rapid H−D exchange, presumably via the enol intermediate, takes place.

The room-temperature ^1H NMR spectrum in CCl_4 is that of **11a** (major) and an enol (δ 18.00) + CO_2Me signals (minor). In DMSO, the ^1H NMR spectrum is exclusively that of **11a**.

Substituent and Structural Effects. (a) Dissection to the Contributions of the Enol and the Carbonyl Form. Dissection to the effects of the β-substituents on the enols and the ketones is obtained from the calculated ΔH values of isodesmic transfer reactions of the two β-substituents in **1** and **2** to CH_4 (eqs 3a−7a) or ethylene (eqs 3b−7b). Both series lead to similar conclusions, and only those with ethylene are discussed. Positive ΔH values mean that the substituted species is more stable than the parent system. Enol **11b** is stabilized by ca. 29 kcal/mol (eq 3b), and amide **11a** and imine **11c** are destabilized by ca. 5 and 7 kcal/mol, respectively (eqs 4b and 5b). Hence, the relative stabilization of **11b** arises from a mild amide destabilization (14% of the effect) and a major (86% of the effect) enol stabilization. The destabilization of **11a** and **11c** probably reflects repulsion between the dipoles of the ester carbonyls and the amido carbonyl of **11a** or the imino nitrogen of **11c**. **11a** and **11c** display similar electronic effects, since NHPh replaces OH and simultaneously C═O replaces C═NPh.

A smaller enol stabilization (16.5 kcal/mol, 64% of the effect) superimposed on a larger ester destabilization (ca. 9 kcal/mol, 32% of the effect) is calculated for ester **13**. The 9.6 kcal/mol higher stabilization of the enol of anilide **11a** (5.7 kcal/mol) than that of the ester **13b** (−3.9 kcal/mol) agrees with the higher K_{enol} values of enols $H_2C{=}C(OH)X$. The ΔH values of 29.6 (OMe) and 27.6 (NH_2) kcal/mol are due to enol stabilizations of 2.5 (NH_2) and 3.6 (OMe) kcal/mol and ketone stabilizations of 17.0 and 20.1 kcal/mol, respectively.[7a] Hence, two β-ester groups affect strongly the contribution of both species. The $MeCONH_2 \rightleftharpoons MeC(OH){=}NH$ equilibrium favors the imine by 12.8 kcal/mol, whereas **11c** is disfavored by 20.2 kcal/mol compared with the amide isomer.

(b) Relative Stabilities and K_{enol} Values. Enol **7** is highly stable compared with isomer **8**. A lower limit for K_{enol} is ca. 50, assuming that 2% of **8** could have been observed, but the value is much higher since from Chart 1 K_{enol} (gas phase) $\approx 10^{10.8}$. Even if the value will be reduced somewhat in $CDCl_3$ (vide infra), it will still be the highest obtained so far. Enol **7** is relatively much more stable than enols of **11** and **13** and those of other anilides **1**, X = NHPh with R^1, R^2 = CN, NO_2, CO_2R.[29] The K_{enol} value for **11** in $CDCl_3$ is much lower: <0.05. The calculated gas-phase K_{enol} value is 100 for **11** and 5×10^{-4} for **13**.

$K_{enol} = K_a^K/K_a^E$, where K_a^E and K_a^K are the acidities of the enol and keto forms, respectively. The higher the C_β-substitutent negative charge delocalizing ability, the higher is K_a^K. The effect of β-substituents on K_a^E is smaller, as reflected in the pK_a^K, pK_a^E values of $R^1R^2C{=}C(OH)_2$: 27, 7 ($R^1 = R^2 =$ H), 22, 6.6 (R^1 = Ph, R^2 = OH), 9.7, 1.3 ($R^1R^2C{=}$ = cyclopentadienylidene), and 8.2, 1.0 (R^1 = Ph, R^2 = CN), respectively.[30]

MA (pK_a = 4.83 (H_2O), 7.32 (DMSO))[31] is a much stronger acid than $CH_2(CO_2Me)_2$ (pK_a(DMSO) = 15.87)[31b] or dimedone (pK_a(DMSO) = 11.24).[31] MA enolizes <1% in solution or in the solid.[32] We assume that CONHPh substitution does not change enormously the pK_a ratio of the two parent carbon acids, unless steric hindrance to planarity is important, and that similar factors affect $pK_a^K(R^1R^2CH_2)$ and $pK_a^K(R^1R^2CHCONHPh)$. Hence, the ΔpK_{enol} of two acid derivatives **2** will be as large as the ΔpK_a^K of $R^1R^2CH_2$. It is encouraging that the 11.7 kcal/mol difference in pK_a(DMSO) values between MA and $CH_2(CO_2Me)_2$[31] and in the calculated ΔG values corresponding to the K_{enol} values are identical.

The pK_a difference of MA and $CH_2(CO_2Me)_2$ was ascribed to a stereoelectronic effect. The high acidity of MA is due to the ring-enforced high ground-state *E* conformation of the ester groups.[31] MO calculations on simple model carboxylic groups for MA and $CH_2(CO_2Me)_2$[33,34] indicate a higher acidity of the *E* conformer, mainly ascribed to the greater Me−O/C═O dipole−dipole interaction than in the *Z* conformer.[33] This interaction in MeOAc is attractive in the Z conformer and absent in the *E* conformer, and vanishes in their anions.[34] From similar considerations on **7** and **11**, the large ΔpK_{enol} value is mainly due to a large ΔpK_a^K difference.

(c) The Importance of Hydrogen Bonding. Two features characterize strong H-bonds:[26] (a) a short OO distance of the OHO system (the H-bond energy rises sharply as the distance decreases and is appreciable at 2.4 Å) and (b) a high δ(OH) value. For the observable enols $CH_2(COR)_2$, R = Me, Ph δ-(OH) > 16. For solid **7**, the O1−O2 distance is 2.46 Å and δ(OH) = 15.70 in $CDCl_3$. Calculated OO distances in **11b**, **13b** and **12a, 12b**, and **12d** are 2.42, 2.42, and 2.41−2.55 Å, and δ(OH) of **11b** in $CDCl_3$ is 17.05. Although the H-bonds are not entirely linear, both criteria for a strong H-bond are fulfilled. Such bonds may stabilize the enols by >10 kcal/mol.[26] Stabilization by the longer and weaker NHO bond is probably compensated by a similar contribution in the amide. Hence, an appreciable fraction (>0.3) of the increase in K_{enol} over the parent system arises from this effect.

Solvent Effect on the Amide ⇌ Enol Equilibria. The solvent effect on the calculated **12a**/**12b** energy difference is minor: **12a** is more stable than **12b** by 1.3 (gas phase, ϵ = 1.0), 1.5 (heptane, ϵ = 1.92), and 2.1 (water, ϵ = 78.4) kcal/mol; i.e., K_{enol} slightly increases on decreasing the polarity. This is consistent with the observed spectral changes. In the low-polar $CDCl_3$, $Cl_2CDCDCl_2$, and CCl_4, the spectra are those of enol **7**. In the more polar DMSO, the spectra cannot exclude a small amount of an amide species. For **11**, both the amide (95%) and enol(s) are observed in $CDCl_3$ or CCl_4, but the enol is not observed in DMSO-d_6; i.e., K_{enol} seems higher in the chlorinated solvents. A similar effect was observed for 1,3-dicarbonyl compounds; e.g., for $CH_2(COMe)_2$, the enol comprises 97.6, 94.6, 82.6, 52.9, and 12.9% in the gas phase, in CCl_4, in $CHCl_3$, in MeCN, and in water, respectively,[9] and the trend for acetoactanilide is similar.[9] The explanation is that the H-bonded

(30) Andraos, J.; Chiang, Y.; Kresge, A. J.; Popik, V. V. *J. Am. Chem. Soc*. **1997**, *119*, 8417.

(31) (a) Arnett, E. M.; Harrelson, J. A., Jr. *J. Am. Chem. Soc.* **1987**, *109*, 809. (b) Arnett, E. M.; Maroldo, S. L.; Schilling, S. L.; Harrelson, J. A. *J. Am. Chem. Soc*. **1984**, *106*, 6759.

(32) (a) Eigen, M.; Ilgenfritz, G.; Kruse, W. *Chem. Ber*. **1965**, *98*, 1623. (b)Arnett, E. M.; Harrelson, J. A. *Gazz. Chim. Ital*. **1987**, *117*, 237. (c) Pluger, C. E.; Boyle, P. D. *J. Chem. Soc., Perkin Trans. 2* **1985**, 1547.

(33) Wang, X.; Houk, K. N. *J. Am. Chem. Soc*. **1988**, *110*, 1870.

(34) Wiberg, K. B.; Laidig, K. E. *J. Am. Chem. Soc*. **1988**, *110*, 1872.

enol is less polar than the amide form, and hence the latter is more solvated and stabilized, thus reducing K_{enol}.[9,35]

Deuterium-Induced ^{13}C Chemical Shifts. The observed deuterium-induced ^{13}C chemical shifts on the C_β-D/C_β-H of the amide form or the C_α-OD/C_α-OH of the enol form could help to distinguish these structures. However, this tool, which was applied to 2,2-ditipylethene-1,1-diols[6c] and for intramolecularly H-bonded enols and related systems,[36] was not an unequivocal probe in our systems. In the mixture of mono- and dideuterated species (O−D, N−D, O,N−d_2), many deuterium-induced shifts of mostly ca. 0.1 ppm were observed for both C_α and more remote carbons of **7** and **10c**.

Conclusions. Several conclusions are drawn: (a) Two strongly EWGs can effectively increase K_{enol} by the combination of a stabilizing push−pull interaction of the enol and a simultaneous destabilization of the "keto" form. (b) In favorable cases, a solid enol of an amide is obtained. (c) In $CDCl_3$ solution, enol **7** is the major or exclusive species, and in **11** the enol **11b** is a minor but observable species. In DMSO-d_6 or CD_3CN, the enolic hydrogen is not observed at room temperature, the major species resembles that observed in $CDCl_3$, but the percentage of the enol is lower and a rapid amide ⇌ enol exchange may occur. (d) Enolization at an RCO site may predominate over that at a COX carbonyl. (e) $CH(EWG)_3$ systems such as **7** or **11** decompose on raising the temperature. (f) The push−pull character of the enols is reflected in their spectral parameters. (g) Calculations show a much higher stability of the *syn* than of the *gauche* conformer of enols. These conclusions indicate that a systematic study with more systems is worthwhile. We are involved now with such a study.

Experimental Section

General Methods. Melting points, FT IR spectra, NMR spectra, and low- and high-resolution mass spectra were recorded as described previously.[6b] The solid-state CPMAS ^{13}C NMR measurements at 125.76 MHz were performed on a Bruker DMX-500 digital FT NMR spectrometer equipped with a BL-4 CPMAS probehead and a high-resolution/high-performance (HPHP) ^1H preamplifier for solids. A solid glycine standard (C═O at δ 176.03) was used for calibration. A vacptppm variable-amplitude cross-polarization with a two-pulse phase modulation broad-band proton decoupling) pulse program was used for the spectrum. A vacptppmnqs (nqs = nonquaternary and nonmethyl signal supression) pulse program was utilized to afford spectral editing, giving "quaternary-/methyl-only" spectra. Samples were placed in 4-mm zirconia rotors and spun at a rate of 11.0 MHz.

Solvents and Materials. Meldrum's acid, dimedone, phenyl isocyanate, diethyl benzylmalonate, and diethyl phenylmalonate were purchased from Aldrich. Commerical deuterated solvents for NMR spectroscopy (Aldrich) and solvents for chromatography were used without further purification.

Diethyl Benzylmalonate. ^1H NMR ($CDCl_3$): δ 1.18 (6H, 2t, 2Me), 3.20 (2H, d, CH_2), 3.64 (1H, m, CH), 4.12 (4H, q, $2CH_2$), 7.16−7.28 (5H, m, Ph).

Diethyl Phenylmalonate. ^1H NMR ($CDCl_3$): δ 1.24 (6H, t, 2Me), 4.20 (4H, 2q, CH_2), 4.61 (1H, s, CH), 7.32−7.40 (5H, m, Ph).

Dimethyl triphenylmethylmalonate was available from a previous work. ^1H NMR ($CDCl_3$): δ 3.47 (6H, s, 2Me), 5.38 (1H, s, CH), 7.18−7.36 (15H, m, Ph).

5-(α-Phenylamino-α′-hydroxy)methylene Meldrum's Acid (7). To a solution of Meldrum's acid (1.5 g, 10.4 mmol) in dry DMF (10 mL) was added Et_3N (2.8 g, 20.8 mmol) and the mixture was stirred for 5 min at room temperature. PhNCO (1.13 mL, 10.4 mmol) was added, and stirring was continued for 30 min. The bright orange solution was poured into 2 N HCl ice-cooled aqueous solution (100 mL). The white solid precipitate was filtered, washed with cold water, and dried, giving 2 g (74%) of crude **7**. Crystallization (EtOAc−petroleum ether, 60−80 °C) gave pure **7**, mp 109−110 °C. ^1H NMR ($CDCl_3$, 240 K): δ 1.78 (6H, s, Me), 7.27 (1H, t, *p*-Ph-H), 7.35−7.40 (2H, t, C_m), 7.45 (2H, d, C_o), 11.14 (1H, br s, NH), 15.63 (<1H, br s, OH). The signal at δ 15.63 disappeared immediately on shaking the solution with D_2O. The compound is stable in MeOH for 4 h at room temperature. ^1H NMR (CCl_4/<10% $CDCl_3$): δ 1.78 (6H, s, Me), 7.20−7.48 (5H, m, Ph), 11.20 (1H, br s, NH), 15.94 (1H, br s, OH). ^1H NMR (rt, CD_3CN): δ 1.74 (6H, s, Me), 7.27−7.49 (5H, m, Ph), 11.03 (1H, br s, NH). ^1H NMR (220 K, CD_3CN): δ 1.68 (6H, s, Me), 7.24−7.40 (5H, m, Ph), 7.50−7.57 (4 small s), 10.95 (1H, NH), 11.4 (small s), 15.70 (1H, s, OH). ^1H NMR (DMSO): δ 1.69 (6H, s, Me), 2.50 (small, m), 7.26−7.49 (5H, m, Ph), 10.99 (1H, br s, NH). ^{13}C NMR ($CDCl_3$): δ 26.02 (Me), 73.50 (C_β), 104.80 (*C*Me_2), 121.89 (d of m, J = 163 Hz, C_m), 126.33 (d of t, J = 163 Hz, C_p), 129.26 (d of d, J = 163 Hz, C_o), 134.67 (C_{ipso}), 164.07 (small, C═O), 168.83 (small, C═O), 170.49 (C_α). ^{13}C NMR (CCl_4, external C_6D_6 reference): δ 28.17, 75.16, 106.04, 123.47, 127.63, 130.93, 137.27, 171.03. ^{13}C NMR (DMSO, coupled): δ 25.59 (q of m), 73.67 (s), 104.61 (complex m), 122.77 (d of m), 126.19 (d of t), 129.04 (d of d), 134.74 (t of m), 166.48 (s), 168.37 (s). ^{13}C NMR ($CDCl_3$, shaken with 1:1 D_2O/H_2O): δ 26.18, 73.49, 104.92, 122.00/122.10, 126.38, 129.21, 134.61 + 134.69, 164.15, 168.82 + 168.89, 170.44. ^{13}C NMR (rt, DMSO-d_6, shaken with 1:1 D_2O/H_2O): δ 26.22, 75.0, 104.71, 119.20+119.30 122.79, 123.03, 126.39, 129.56 + 129.86, 135.36, 139.86, 167.26. The + sign indicates that pairs of signals around it are due to isotope-induced shift. IR ($CHCl_3$, ν_{max}, cm^{-1}): 3179 (w, br, OH), 1697 (C═O, s), 1651 (C═O, s). Microanalysis. Calcd for $C_{13}H_{13}NO_5$: C, 59.31; H, 4.98; N, 5.32. Found: C, 59.16; H, 4.92; N, 4.85. HRMS: calcd for $C_{13}H_{13}NO_5$ 263.0794, found 263.0786. *m*/*z* (abundance relative to *m*/*z* 205, assignment): 263 (44, M), 205 (100%, M − Me_2CO), 159 (13%, M − CNHPh), 133 (35%, C_2(OH)NHPh). MS(EI): *m*/*z* 93 (100%, $PhNH_2^+$).

Crystallographic Data for 7. $C_{13}H_{13}NO_5$; space group $P2_1/n$; a = 18.058(3) Å, b = 12.320(2) Å, c = 5.644(1) Å; β = 90.24(1)°; V = 1255.6 Å^3; Z = 4; ρ_{calcd} = 1.39 g cm^{-3}; μ(Mo Kα) = 1.01 cm^{-1}; no. of unique reflections, 2336; no. of reflections with $I \geq 3\sigma_I$, 1522; R = 0.055; R_w = 0.082.

2-Hydroxy-4,4-dimethyl-5-oxo-*N*-phenylcyclohexenecarboxamide (10c). To a stirred solution of dimedone (1 g, 7.14 mmol) in dry DMF (7 mL) is added Et_3N (1.98 g, 14.29 mmol), followed by PhNCO (0.77 mL, 7.14 mmol). The mixture is stirred for 40 min at −10 to −12 °C and then poured into 2 N aqueous HCl solution (80 mL), and the precipitated solid is filtered, washed with cold water, and crystallized (EtOAc−petroleum ether, 60−80 °C) to a white solid (1.2 g, 48%), mp 84−5 °C. ^1H NMR ($CDCl_3$, rt): δ 1.15 (6H, s, 2Me), 2.41 (2H, s, CH_2), 2.53 (2H, s, CH_2), 7.17 (1H, t, *p*-Ph-H), 7.35 (2H, t, *m*-Ph-H), 7.56 (2H, d, *o*-Ph-H), 11.77 (1H, br s, NH), 17.82 (1H, br s, OH). The δ 17.82 signal rapidly exchange in D_2O. At 223 K, δ(OH) = 18.0 (<1H). δ(DMSO-d_6): 1.03 (6H, s, Me), 2.45 (2H, s, CH_2), 2.51 (2H, s, CH_2), 7.17 (1H, t, *p*-Ph-H), 7.38 (2H, m, *m*-Ph-H), 7.56 (2H, d, *o*-Ph-H), 11.76 (1H, br s, NH), 17.46 (1H, br s, OH). ^{13}C NMR ($CDCl_3$, 223 K): δ 27.74 (q, Me), 30.65 (s, CMe_2), 44.65 (t, CH_2), 50.44 (t, CH_2), 101.72 (s, C_β), 120.72 (d of m, C_m), 124.62 (d of t, C_p), 128.73 (d of d, C_o), 136.00 (t, ^3J = 9 Hz, C_{ipso}), 168.83 (C_α), 194.17 (q, J = 8 Hz, C═O), 197.41 (t, ^3J = 6 Hz, C═O). The room-temperature spectrum is similar. ^{13}C NMR (DMSO-d_6): δ 27.13, 30.48, 44.22, 50.30, 101.70, 120.86, 124.82, 128.97, 136.21, 168.90, 194.04, 197.34. IR (ν_{max}, cm^{-1}, Nujol): (br m, OH), 3186 (vw, br), 1720 (s, C═O), 1654 (C═O, w). IR (ν_{max}, cm^{-1}, $CHCl_3$): 3318, 3281 (m, OH), 1712 (w), 1654 (C═O, s). Microanalysis. Calcd for $C_{15}H_{17}NO_3$: C, 69.48; H, 6.61; N, 5.40. Found: C, 69.27; H, 6.59; N, 5.49.

Crystallographic Data for 10c. $C_{15}H_{17}NO_3$; space group $P2_1/c$; a = 12.061(2) Å, b = 12.752(2) Å, c = 18.370(4) Å; β = 104.45°; V = 2736(1) Å^3; Z = 4; ρ_{calcd} = 1.26 g cm^{-3}; μ(Mo Kα) = 0.82 cm^{-1}; no. of unique reflections, 5065; no. of reflections with $I \geq 3\sigma_I$, 2911; R = 0.055; R_w = 0.074.

Reaction of Dimethyl Malonate with Phenyl Isocyanate. A solution of dimethyl malonate (1 g, 7.6 mmol), PhNCO (0.82 mL, 7.6

(35) Floris, B. In ref 1, Chapter 4, p 147.

(36) (a) Hansen, P. E.; Bolvig, S.; Duus, F.; Petrova, M. V.; Kawecki, R.; Kozerski, L. *Magn. Reson. Chem.* **1995**, *33*, 621. (b) Kozerski, L.; Kawercki, R.; Krajewski, P.; Kwiecien, B.; Boykin, D. W.; Bolvig, S.; Hansen, P. E. *Magn. Reson. Chem.* **1988**, *36*, 921.

mmol), and Et_3N (2.1 mL, 15.14 mmol) in dry DMF (7 mL) was heated for 2.5 h at 55 °C and then stirred at room temperature for 14 h. The mixture was poured into a cooled 2 N aqueous HCl solution (90 mL) and extracted with EtOAc (125 mL), which was washed with water (3 × 40 mL), dried (Na_2SO_4), and evaporated. Chromatography of the gummy residue (1.95 g) over silica gel with 25% EtOAc/petroleum ether eluent gave a solid (1.03 g, 54%) which was recrystallized from EtOAc/petroleum ether. The first precipitated crystals (20 mg), mp 238−240 °C, were identified by X-ray crystallography as *N*,*N*′-diphenylurea, mp 240 °C. The main fraction, mp 98−100 °C, is **11**. ^{1}H NMR ($CDCl_3$): δ 3.81 (0.33H, s, CO_2Me of **11b**), 3.86 (6H, s, CO_2Me), 4.49 (1H, s, CH), 7.14 (1H, t, *p*-Ph-H), 7.37 (2H, t, *m*-Ph-H), 7.56 (2H, d, *o*-Ph-H), 9.26 (ca 1H, br s, NH), 17.05 (0.05H, s, OH of **11b**). The signals at 4.49, 9.25, and 17.05 ppm disappeared rapidly with D_2O. ^{1}H NMR (CCl_4, external C_6D_6): δ 4.64 (s, Me), 4.74 (s, Me), 5.21 (s, CH), 7.97 (m), 8.17 (t), 8.33 (d), 8.45 (d) [all Ph-H], 10.02 (s, NH), 12.93 (br s, NH), 18.00 (s, OH). ^{1}H NMR (DMSO-d_6): δ 3.71 (6H, s, CO_2Me), 4.77 (1H, s, CH), 7.08 (1H, t, *p*-Ph-H), 7.32 (2H, t, *m*-Ph-H), 7.52(2H, d, *o*-Ph-H), 10.33 (ca. 1H, br s, NH). ^{1}H NMR (CD_3CN, rt): δ 3.83 (3H, s, Me), 4.58 (0.45H, br, CH), 7.16−7.55 (5H, m, Ph), 7.28 (0.3H, br s, Ph-H), 8.30 (0.16H, br s, Ph-H), 8.85 (0.4H, br s, Ph-H). ^{13}C NMR (uncoupled $CDCl_3$): δ 53.60 (Me, q), 59.18 (CH, d), 120.15 (C_p, d of m), 124.93 (C_m, d of t), 128.98 (C_o, d of d), 137.05 (C_{ipso}), 159.64 (C_α, d of d), 166.08 (CO, hept, J = 4.2 Hz).

At 220 K in the coupled spectrum in $CDCl_3$, new signals (δ 41.17, t) and (δ 53.83, q) (7% of the intensities) accompany the corresponding major signals. The aromatic signals at 119.69, 124.81, 128.86, and 136.57 ppm were accompanied by a new overlapping multiplet at ca. 119.86, 124.52, 128.90 and 136.84 ppm, with 10% of their intensity. The CH signal at δ 58.83 displays no satellite signal, but new signals appear at 163.31, 169.60, 169.95, and 174.73 with ca. 10% of the intensity of the neighboring main signals. ^{13}C NMR (uncoupled, DMSO-d_6, rt): δ 52.78 (t, Me), 60.46 (d, CH), 118.08 (small, overlapping), 119.02 (d of m, C_m), 123.92 (overlapping, d of t, C_p), 128.71 (d of d, C_o), 128.84 (d of d, small), 138.26 (t, J = 9.4 Hz, C_{ipso}), 160.94 (d of d, J = 9; 2.7 Hz, CONHPh), 165.16 (sextet, J = 4 Hz, COOMe). IR (ν_{max}, cm^{-1}, $CHCl_3$): 3332 (br vw, OH) 1751 (m, C═O), 1697 (m, C═O), 1613. IR (Nujol) 3326 (br, m), 1747 (s), 1691 (s), 1607 (s). Microanalysis. Calcd for $C_{12}H_{13}NO_5$: C, 57.37; H, 5.22; N, 5.58. Found: C, 57.67; H, 5.21; N, 5.36.

Crystallographic Data. $C_{12}H_{13}NO_5$; space group $P2_1/c$; a = 9.908(4) Å, b = 44.385(8) Å, c = 9.248(4) Å; β = 107.97(3)°; V = 3868(2) Å^3; Z = 12, ρ_{calcd} = 1.29 g cm^{-3}, μ (Cu Kα) = 8.65 cm^{-1}, No. of unique reflections 5716, No. of reflections with $I \geq 3\sigma_I$ 2911. R = 0.058, R_w = 0.086.

Acknowledgment. We are indebted to Mr. Niv Papo for preliminary experiments, to Prof. M. Kaftory for his help with the CSDB, to Dr. Shmuel Cohen for the crystallographic determination, to Prof. Robert Glaser for the solid ^{13}C NMR spectra, and to the Israel Science Foundation for support.

Supporting Information Available: Tables of bond lengths and angles, position and thermal parameters, stereoviews of **7**, **10c**, and **11a**, solid-state structures and ^{1}H and ^{13}C NMR plots of **11a**, B3LYP/6-31G** energies of various species, and dihedral angles of **12a**−**e** (PDF). This material is available free of charge via the Internet at http://pubs.acs.org.

JA992059F